Inhibition of Melittin Activity Using a Small Molecule with an Indole Ring

Kanemitsu, Sayuki ; Morita, Kenta ; Tominaga, Yudai ; Nishimura, Kanon ; Yashiro, Tomoko ; Sakurai, Haruka ; Yamamoto, Yumemi ; Kurisaki, Iku…

(Citation)
Journal of Physical Chemistry B,126(31):5793-5802

(Issue Date)
2022-08-11

(Resource Type)
journal article

(Version)
Accepted Manuscript

Inhibition of Melittin Activity Using a Small Molecule with an Indole Ring

Sayuki Kanemitsu,[†] Kenta Morita,[†] Yudai Tominaga,[†] Kanon Nishimura,[†] Tomoko Yashiro,[†] Haruka Sakurai,[§] Yumemi Yamamoto, [§] Ikuo Kurisaki, [‡] Shigenori Tanaka,[‡] Masaki Matsui,[†] Tooru Ooya, [†] Atsuo Tamura[§] and Tatsuo Maruyama[†,] [¶]*

[†]Department of Chemical Science and Engineering, Graduate School of Engineering, Kobe University, 1-1 Rokkodai, Nada-ku, Kobe 657-8501, Japan.

[‡]Department of Computational Science, Graduate School of System Informatics, Kobe University, 1-1 Rokkodai, Nada-ku, Kobe 657-8501, Japan.

[§]Graduate School of Science, Department of Chemistry, Kobe University, 1-1 Rokkodai, Nada-ku, Kobe 657-8501, Japan.

[¶]Research Center for Membrane and Film Technology, Kobe University, 1-1 Rokkodai, Nada-ku, Kobe 657-8501, Japan.

KEYWORDS. D-amino acids, indole derivatives, activity inhibition, π–π interaction, toxic peptide

ABSTRACT

We investigated D-amino acids as potential inhibitors targeting L-peptide toxins. Among the L- and D-amino acids tested, we found that D-tryptophan (D-Trp) acted as an inhibitor of melittin-induced hemolysis. We then evaluated various Trp derivatives and found that 5-chlorotryptamine (5CT) had the largest inhibitory effect on melittin. The indole ring, amino group, and steric hindrance of an inhibitor played important roles in the inhibition of melittin activity. Despite the small size and simple molecular structure of 5CT, its IC_{50} was approximately 13 μg/mL. Fluorescence quenching, circular dichroism (CD) measurements, and size-exclusion chromatography revealed that 5CT interacted with Trp19 in melittin and affected the formation of the melittin tetramer involved in hemolysis. Molecular dynamics simulation of melittin also indicated that the interaction of 5CT with Trp19 in melittin affected the formation of the tetramer.

INTRODUCTION

Inhibition of the activities of toxic biomolecules and proteins involved in disease has been extensively studied. Many effective inhibitors have been discovered fortuitously and systematically using huge compound libraries. In silico design of a novel inhibitor has become another powerful tool for drug discovery in the last two decades, in which an inhibitor acts on a protein according to a lock-and-key model.[1-5] Although proteins were long considered to have fixed or ordered three-dimensional structures, studies have shown that many proteins have intrinsically disordered regions in their molecular structures, known as intrinsically disordered proteins (IDPs). Since the end of the last century, IDPs have been recognized as important in biochemistry and medical science.[6-10] The proportion of disordered regions in the sequences of proteins produced in eucaryotes is 20% to 30% on average.[7] Some IDPs (e.g., amyloid β and α-synuclein) are involved in diseases.[11-13] The disordered structure in disease-related proteins makes it difficult to develop an effective inhibitor as a potential medicine. Therefore, to discover inhibitors that target disease-related IDPs, it is necessary

to develop strategies that differ from the approach used in conventional drug discovery.[14]

Since the late 20th century, D-amino acids and peptides incorporating D-amino acids have been found in various living systems. Numerous investigations have revealed the important roles of D-amino acids in living systems. Among them, Losick et al. found that D-amino acids inhibit the development of biofilms with amyloid-like characteristics.[15, 16] Thakur et al. reported that D-phenylalanine (D-Phe) can disrupt the formation of amyloid fibrils comprising L-phenylalanine (L-Phe).[17] They proposed the use of D-Phe as a modulator of amyloid formation in phenylketonuria disease. These pioneering studies indicate that D-amino acids and their derivatives can modulate the function of IDPs and peptides with labile conformations, which can be applied to the rational design of novel inhibitors targeting IDPs and peptides.

Melittin is the main toxic component of honeybee venom, which comprises 26 amino acid residues.[18] The labile conformation of melittin is sensitive to solution conditions (e.g., ionic strength, pH, and solution concentration).[19] Indeed, Knóppel et al. reported that melittin has a random structure in dilute aqueous solution, while it has an α-helical structure in methanol solution and when it is embedded in a lipid membrane.[20-22] Four (or more) melittin monomers can self-assemble to form a tetramer (or oligomer), which becomes a transmembrane pore on cell membranes, leading to cytolysis and hemolysis.[23-27] Despite the various studies on melittin, there are limited studies on melittin inhibitors (peptide-based inhibitor[28-35] and polymer-based inhibitor[36-40]), likely because of the labile conformation of melittin. Inspired by the above studies, we conjectured that a novel inhibitor with controlled chirality can be designed by considering the primary structure of melittin. In the present study, we adopted melittin as a model functional and labile peptide and attempted to inhibit melittin function (hemolytic activity) using D-amino acids and their derivatives.

METHODS

Materials

L- and D-Amino acids and their derivatives (unless otherwise stated) were purchased from BLD Pharmatech Ltd. (Shanghai, China), Fujifilm Wako Pure Chemical Co., Ltd. (Osaka, Japan), Nacalai Tesque, Inc. (Kyoto, Japan), Tokyo Chemical Industry (Tokyo, Japan), and Watanabe Chemical Industry (Hiroshima, Japan). All the D- and L-amino acids were more than 98% pure. Tryptamine was purchased from Fujifilm Wako Pure Chemical Co., Ltd. (Osaka, Japan). 3-Indoleacetic acid, indole, 5-hydroxytryptamine hydrochloride (serotonin) were purchased from Nacalai Tesque, Inc. 5-Chloroindole-3-acetic acid was purchased from Kanto Chemical Co., Inc. (Tokyo, Japan). 5-Fluoro-D-tryptophan was purchased from Chem-Impex International, Inc. (Wood Dale, IL). 5-Chloro-D-tryptophan was purchased from Amatek Chemical Co., Ltd. (Jiangsu, China). Melittin from honeybee venom (≥85%) was purchased from Sigma-Aldrich (St. Louis, MO). Dipeptide and melittin conjugated with carboxytetramethylrhodamine (TAMRA, > 90% purity)) at the N-terminus (TAMRA-melittin) was purchased from Cosmo Bio Co., Ltd (Tokyo, Japan). Bovine blood was purchased from Japan Bio Serum (Hiroshima, Japan). Dulbecco's phosphate buffered saline (D-PBS buffer) was purchased from Nacalai Tesque, Inc. D2O was purchased from Tokyo Chemical Industry. Pentaerythritol tetra(aminopropyl) polyoxyethylene (also known as Sunbright PTE-100PA) and 1-palmitoyl-2-oleoyl-*sn*-glycero-3-phosphocholine (POPC) were purchased from NOF Corporation (Tokyo, Japan).

Other chemicals were purchased from Fujifilm Wako Pure Chemical Co., Ltd. High-purity deionized water (Milli-Q water, >15 MΩ·cm) from an Elix-5 system (Millipore, Molsheim, France) was used.

Hemolysis experiments

A melittin solution containing an inhibitor candidate was prepared using D-PBS (pH 7.4). The final concentrations of melittin and the inhibitor candidate in solution were 5 μM and 500 μM, respectively. The pH value of the solution was approximately 7.2. Red blood cells (RBCs) were obtained by centrifuging 1.5 mL of bovine blood at 4600 × g for 5 min at 4°C. After removing the supernatant, 2

mL of D-PBS was added to the precipitated RBCs, and the solution was mixed using a vortex mixer. After centrifuging the solution and removing the supernatant, 2 mL of melittin solution containing an inhibitor candidate was added to the RBCs for hemolysis at 37°C. After 30 min, the solution was centrifuged and the collected supernatant was diluted (if necessary) and transferred to a well of 96-well plates. The absorbance (Abs) at 415 nm of each well was measured using a microplate reader (SH9000, Hitachi High-Technologies Corporation, Tokyo, Japan). The relative hemolytic activity of melittin in the presence of an inhibitor candidate was calculated using the following formula:

$$Relative\ hemolytic\ activity\ [\%] = \frac{Abs\ of\ (melittin + inhibitor)\ [-]\ -\ Abs\ of\ (control)\ [-]}{Abs\ of\ (melittin\ only)\ [-]\ -\ \text{Abs of (control)}\ [-]} \times 100$$

Circular dichroism (CD) spectra

Melittin (20 μM) and 5-chlorotryptamine (5CT, 200 μM) solutions were prepared separately using 10 mM phosphate buffer at pH 7.4. Equal volumes of these solutions were mixed with each other. POPC was dispersed in phosphate buffer using an ultrasonicator to prepare a liposome solution with a concentration of 100 μM POPC. The liposome solution was mixed with the solution containing melittin and 5CT in equal volumes. The final concentration of melittin, 5CT, and POPC were 5 μM, 50 μM, and 50 μM, respectively. CD measurements were repeated 8 times at 25°C on a Jasco J-725K CD instrument using 10-mm quartz cuvettes.

Attenuated total reflection IR (ATR-IR) spectra

Melittin (200 μM) and 5CT (2 mM) solutions were prepared separately using Milli-Q water. Equal volumes of these solutions were mixed with each other. POPC was dispersed in Milli-Q water using an ultrasonicator to prepare a liposome solution with a concentration of 2 mM POPC. The liposome solution was mixed with the solution containing melittin and 5CT in equal volumes. The final

concentrations of melittin, 5CT, and phospholipids were 50 μM, 500 μM, and 1 mM, respectively. The solution (50 μL) was dropped on an ATR plate, dried for 30 min in a vacuum to prepare a film, and analyzed using lateral and vertical vibrating polarized light on a Thermo Scientific Nicolet iS50 FT-IR spectrometer (Thermo Fisher Scientific, Waltham, MA). The internal reflection element was a 45° ZnSe crystal (VeeMAX III Flat Plate ZnSe 45 Degrees, PIKE Technologies, Madison, WI). Using variable angle specular reflection accessory (VeeMAX III), the light was deflected by rotating the ZnSe polarized plate by 0° and 90° for lateral vibration and vertical vibration, respectively. The measurements were repeated 128 times at 25°C. The background spectrum was collected using the ATR substrate only. The calculations were performed using a Thermo Scientific™ OMNIC™ software.

Size exclusion chromatography (SEC) analysis of melittin solution

Melittin solutions with and without 5CT were prepared using 10 mM D-PBS (pH 7.4). The final concentrations of melittin and 5CT were 500 μM and 1 mM, respectively. The melittin solution was analyzed using an SEC system (PU-980, JASCO, Tokyo, Japan) equipped with a 7.5 × 300 mm SEC column (GF-310 HQ, Showa Denko K.K., Tokyo, Japan), a light scattering detector (miniDAWN TriStar, Wyatt Technology Corporation, Santa Barbara, CA), and a refractive index detector (Shodex RI-101 detector, Showa Denko, Tokyo, Japan) operating at 37°C under a flow rate of 0.5 mL min^{-1}. D-PBS buffer was used as an eluent. Sunbright PTE-100PA (polyethylene glycol 1000) was used as a molecular weight standard.

Confocal laser scanning microscope (CLSM) observation of RBCs with melittin

A TAMRA-melittin solution containing 5CT or D-Trp was prepared using D-PBS (pH 7.4). The final concentrations of TAMRA-melittin and an inhibitor were 5 μM and 500 μM, respectively. The final pH value of the solution was approximately 7.2. RBCs were obtained by centrifuging 1.5 mL of

bovine blood at 4600 × g for 5 min at 4°C. After removing the supernatant, 2 mL D-PBS was added to the precipitated RBCs, and the solution was mixed using a vortex mixer. After centrifuging the solution and removing the supernatant, 2 mL of melittin solution containing an inhibitor was added to the RBCs for hemolysis at 37°C. After 30 min, the RBCs were obtained by centrifuging at 2000 × g for 5 min at 4°C. After removing the supernatant, 2 mL of D-PBS was added to the precipitated RBCs, and the solution was mixed using a vortex mixer. After centrifuging the solution and removing the supernatant, 1 mL of D-PBS was added to the RBCs to prepare a sample for CLSM observation. A sample solution (10 μL) was applied on a cover glass, and another cover glass was laid over the sample. The cover glasses were peeled off and then immersed into methanol for a few minutes. After taking off the cover glasses and drying, CLSM observations were conducted using an FL1000 confocal laser scanning microscope (Olympus, Tokyo, Japan).

Fluorescence spectra analysis

D-PBS solutions containing 50 μM melittin and 5CT at different concentrations (0~1000 μM) were prepared. The fluorescence spectra (excitation 280 nm, emission 275~450 nm) of the solutions were measured using a fluorescence spectrophotometer (FP-8200, JASCO, Tokyo, Japan). The measurements were repeated three times at 25°C. The binding constant (K_b) and the number of binding site (n) were calculated from a Stern–Volmer plot.

^{1}H-NMR analysis

D_2O solutions containing 200 μM melittin and 5CT at different concentrations (0~2 mM) were prepared. ^{1}H-NMR measurements of the solutions were conducted using a Bruker Avance500 spectrometer. The measurements were repeated 256 times at 25°C.

Molecular dynamics simulation

The melittin monomer model was isolated from the crystal structure of a melittin tetramer (PDB ID: 2MLT). 5CT was modeled manually using Winmostar V10,[41] and the structure was optimized using MOPAC6 with the AM1 Hamiltonian.[42] The atomic charges of 5CT were calculated using the antechamber module in AMBER20[43] with the AM1-BCC charge method,[43] while the remaining force field parameters were derived from General Amber Force Field 2 (GAFF2).[44] Four copies of chain A (a melittin monomer) in 2MLT and one hundred copies of 5CT were randomly placed in a 10-nm cubic box and saved as a PDB file using Winmostar V10.

MD simulation was set up and performed under the periodic boundary condition using the GPU version of the PMEMD module in the AMBER20 package[43] in accordance with the SPFP algorithm[45] with NVIDIA GeForce RTX2080Ti. The AMBER force field 14SB,[46] GAFF2, TIP3P water model,[47, 48] and JC ion parameters adjusted for the TIP3P water model[49] were used for melittin, 5CT, water molecules, and ions, respectively. The coordinated model of melittin monomers and 5CT was solvated in a water cubic box with 10-nm edges, and Na^+ and Cl^- were added to create a neutral system with 0.15 M NaCl using the LEaP module. The molecular components are summarized in Table S2. Energy minimization was performed to relax the initial structures. Minimization was carried out by implementing 1000 steps of the conjugate gradient method, followed by another 1000 steps of steepest descent calculation. Before initiating a production run, the temperature and density of the system were equilibrated. All MD simulations were performed with a time step of 2 fs, a nonbonded cutoff length of 10 Å, and a periodic boundary condition. The lengths of bonds attached to hydrogen atoms were fixed using the SHAKE algorithm. The system was heated to 310 K using the Langevin thermostat[50, 51] with a collision frequency γ of 2.0 ps^{-1}. The density of the system was equilibrated three times using a short run (20 ps) with the same settings as the production run. The production run was performed for 2×10^8 steps (400 ns) in the NPT ensemble under 1 bar at 310 K controlled by the Langevin dynamics. The initial coordinates of the system including four melittin monomers with and without 5CTs are provided in supporting information named as ‘melittin+5CT_initial.pdb’ and ‘melittin_initial.pdb’,

respectively. The final coordinates of them are provided as 'melittin+5CT_final.pdb' and 'melittin_final.pdb', respectively.

Molecular coordinates in the systems were visualized using VMD.[52] Trajectory data were analyzed using the CPPTRAJ program in Amber20. The distance between each center of mass to the other three centers of mass in the tetramer was calculated, and the averaged value was used as the average distance between the melittin monomers. A molecular surface area of the melittin oligomer was calculated using the MOLSURF program of CPPTRAJ with a probe radius of 1.4 Å.

a Gly-Ile-Gly-Ala-Val-Leu-Lys-Val-Leu-Thr-Thr-Gly-Leu
-Pro-Ala-Leu-Ile-Ser-Trp-Ile-Lys-Arg-Lys-Arg-Gln-Gln

b

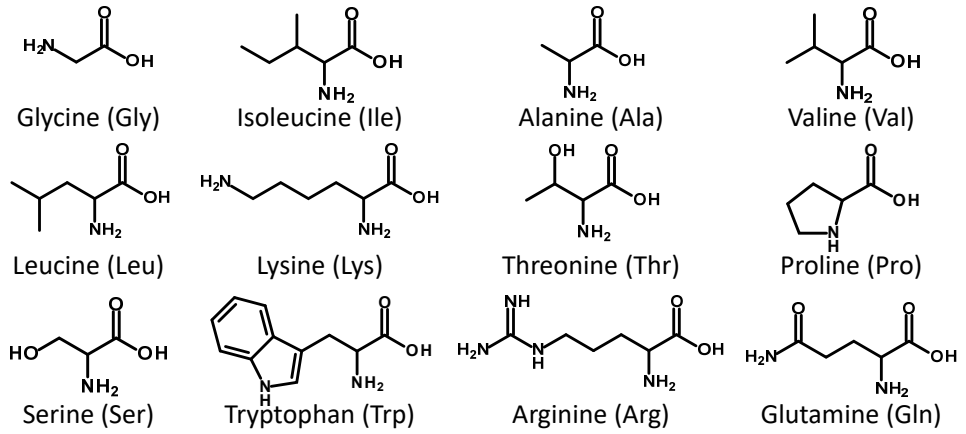

c

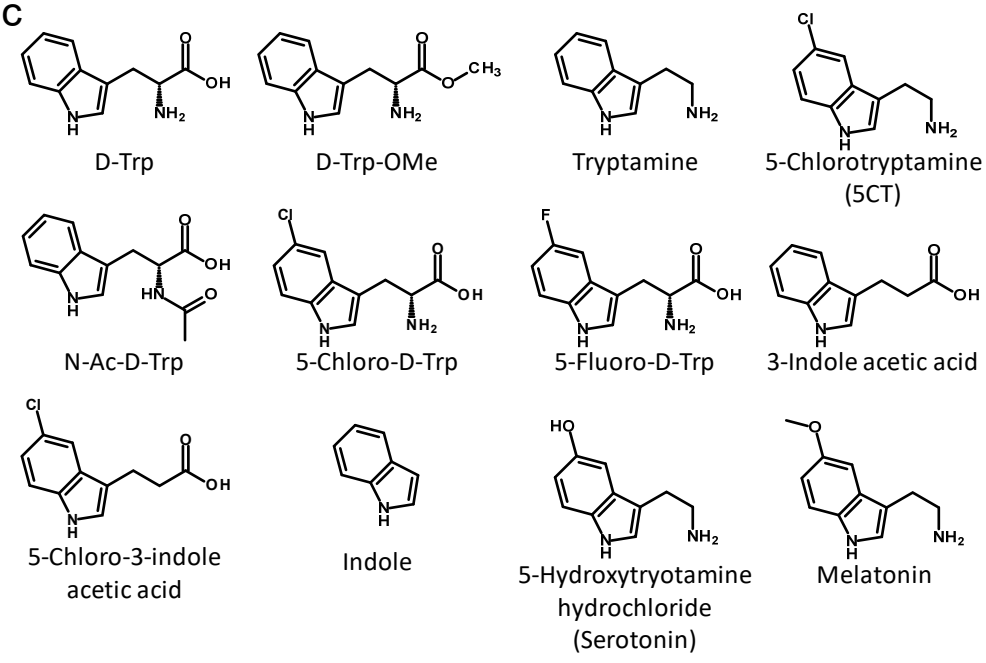

Figure 1 a) Amino acid sequence of melittin. b) Molecular structures of amino acids tested. c) D-Trp and its derivatives used as potential inhibitors targeting melittin in this study.

RESULTS AND DISCUSSION

Screening and evaluation of potential inhibitors targeting melittin

As mentioned in the Introduction, we first examined the inhibitory effect of D-amino acids on the hemolytic activity of melittin. Some studies reported that D-amino acids and D-peptides have the potential to interact with L-peptides, in which π-π stacking and molecular packing were considered to play important roles in the interaction. We selected D-amino acids corresponding to the L-amino acids found in the amino acid sequence of melittin as potential inhibitors targeting melittin (Figure 1a and b). Hemolysis experiments were performed in the presence and absence of D- and L-amino acids to investigate the inhibitory effects of these amino acids on the hemolytic activity of melittin. While the L-amino acids did not exert an inhibitory effect, some D-amino acids exhibited inhibitory effects. Notably, D-Ser enhanced the hemolytic activity of melittin (Figure 2a). Among the D-amino acids showing inhibitory effects, D-tryptophan showed the largest effect (hemolytic activity of only 23% relative to the activity of native melittin). These results indicate that the indole ring and the chirality of tryptophan are involved in the inhibition of hemolytic activity.

On the basis of these results, we examined the inhibitory effects of indole derivatives (Figure 1c). D-tryptophan-methyl ester, tryptamine, and 5CT also showed high inhibitory effects (Figure 2b). The indole ring and free amino group are common features in their molecular structures. The inhibitory effects of tryptamine and 5CT were higher than those of 3-indole acetic acid and 5-chloro-3-indole acetic acid, indicating the importance of the free amino group. Because the hemolytic activity of melittin in the presence of D-Trp, D-Trp-OMe, and tryptamine were 23%, 32%, and 12%, we concluded that the carbonyl group was not involved in the inhibition of melittin. 5CT showed a higher inhibitory effect (only 8% hemolytic activity) than tryptamine. In contrast, 5-chloro-D-Trp and 5-

fluoro-D-Trp did not show remarkable inhibitory effects, which was less than that of D-Trp. These results suggest that the indole ring and amino group play important roles in the inhibition of hemolytic activity.

Because D-Trp and D-Trp-OMe showed inhibitory effects, nine different peptides containing D- or L-Trp were used as potential inhibitors. Figure 2c shows the effect of these dipeptides on the hemolytic activity of melittin. Ser-Trp, Trp-Ile and Trp-Trp (including L- and D-forms) did not exhibit inhibitory effects even when D-Trp was involved. D-Trp-D-Glu and D-Trp-Gly inhibited melittin-induced hemolysis by 60% and 43%, respectively. The D-Trp-containing dipeptide was less effective at inhibiting melittin than the D-Trp monomer, probably because of the steric hindrance of the dipeptides.

We then investigated the effect of 5CT concentration on the hemolytic activity of melittin (Figure 2d). The hemolytic activity decreased with an increase in the 5CT concentration. A 5CT concentration of 100 μM decreased the hemolytic activity by 70%, and a 5CT concentration of 500 μM resulted in a hemolytic activity of 8%. The IC_{50} of 5CT was determined to be 66 μM (13 μg/mL). The reported IC_{50} values of hexapeptide inhibitors range from several μg/mL to more than a dozen μg/mL.[32, 33] Despite the small size and simple molecular structure of 5CT, its IC_{50} was comparable with those of previous studies. 5CT was used as an inhibitor in the following experiments to study the mechanism of melittin inhibition.

In the above experiments, the potential inhibitors were added to a melittin solution before melittin interacted with RBC membranes. Then, we added 5CT to a melittin solution after melittin interacted with RBC membranes. The addition of 5CT decreased the hemolytic activity by approx. 70% (Figure S1), indicating that 5CT affected melittin on the RBC membrane.

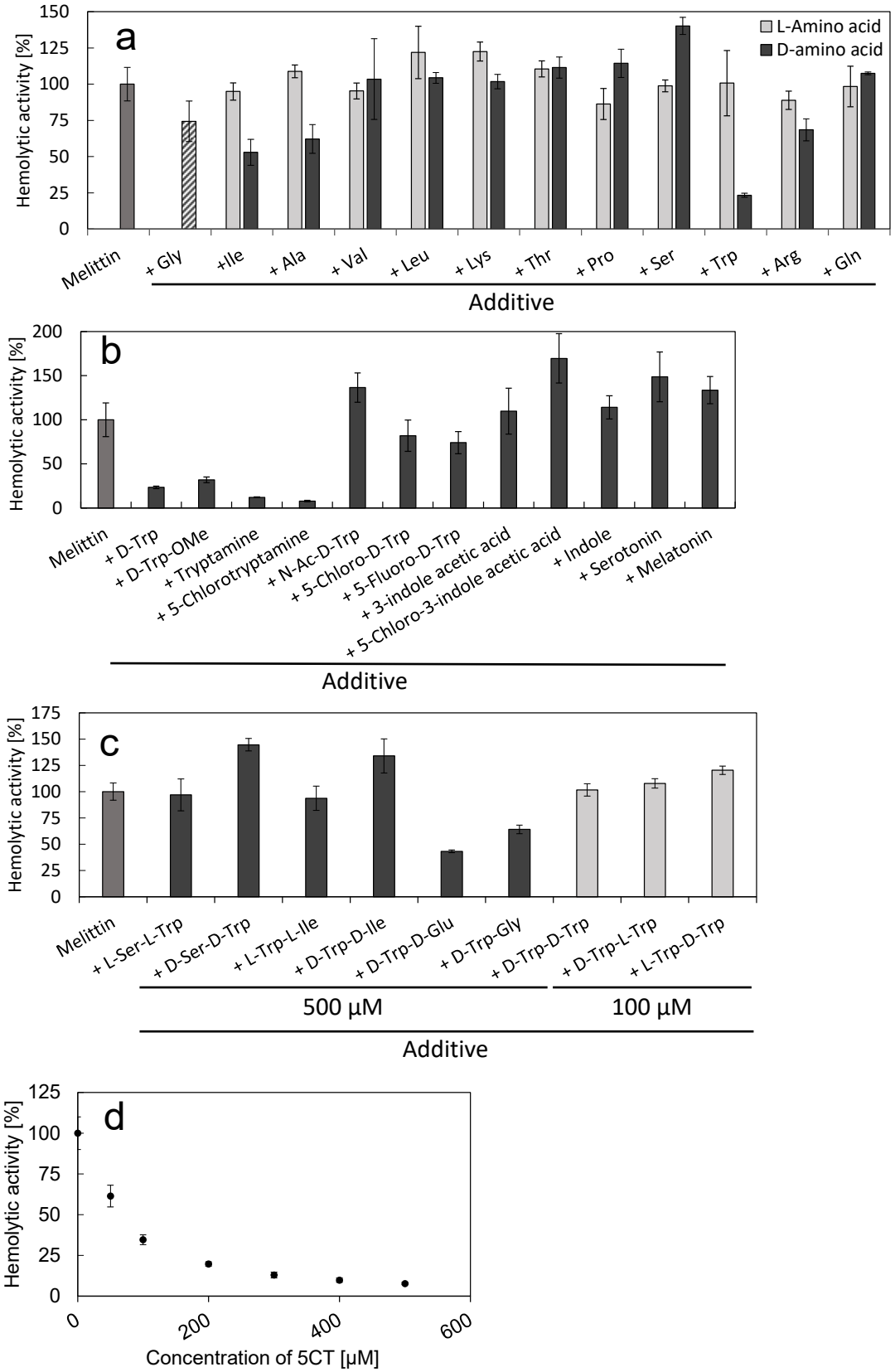

Figure 2 a) Effect of amino acids on the hemolytic activity of melittin. b) Effect of indole derivatives on the hemolytic activity of melittin. The concentrations of melittin and additives were 5 µM and 500

μM, respectively. Hemolytic activity values [%] are relative to the intrinsic hemolytic activity of melittin. c) Effect of Trp-containing dipeptides on the hemolytic activity of melittin. d) Effect of 5-chlorotryptamine (5CT) concentration on the hemolytic activity of melittin. The concentration of melittin was 5 μM. The measurements of the hemolytic activity were carried out in triplicate. Error bars represent the standard deviations.

Structural analysis of melittin with inhibitor

Four molecules (or more) of melittin can self-assemble to form a tetramer (also known as an oligomer) on a cell membrane, which becomes a hole of the cell membrane, thus causing hemolysis.[23-26] To study the inhibition mechanism of 5CT, we measured CD spectra to investigate the formation of α-helices in melittin in the presence of 5CT. In the absence of liposomes, melittin did not form an α-helix, and had random coils at low salt concentrations, which was evidenced by a negative band around at 200 nm (Figure S2). Then, liposomes comprising POPC, instead of RBCs, were added to the melittin solution to mimic the hemolysis environment. Melittin solutions with liposomes exhibited a negative band at 222 nm and also a small negative band at 207 nm (Figure 3a, S2), which indicated the formation of an α-helix.[20] The addition of 5CT to a melittin solution with liposomes changed the CD spectra slightly, which means that 5CT had some effects on the melittin's structure. The two negative bands indicating an α-helix were still observed in the presence of 5CT, which means that melittin still formed an α-helix although in the presence of 5CT. The presence of 5CT seemed not to affect the interaction between melittin and a lipid bilayer, although there was a slight difference in CD spectra of melittin between in the presence and absence of 5CT.

ATR-IR measurements were conducted for melittin in the presence of liposomes. ATR-IR with polarized light provides information on molecular orientation.[53, 54] Studies have shown that phospholipids are orientated perpendicular to an ATR plate and form lipid bilayers when a liposome solution is dried on an ATR plate.[55, 56] Here, we prepared melittin/phospholipid (POPC) samples for

ATR-IR measurements by dropping a melittin solution containing liposomes on an ATR plate and subsequently drying the substrate.

Figure 3b shows the IR spectra of melittin/phospholipid obtained by subtracting the absorption spectra of lateral-vibrating polarized light from those of vertical-vibrating polarized light. Melittin exhibited an absorbance peak at approximately 1650 cm^{-1} both in the absence and presence of 5CT, indicating that the C=O group in melittin molecules absorbed vertical-vibrating polarized light, not lateral-vibrating polarized light. These results indicated that melittin molecules were oriented perpendicular to the membrane in the absence and presence of 5CT.[53, 57] Although 5CT inhibited the hemolytic activity of melittin, 5CT might not affect the molecular orientation of melittin in a lipid membrane.

SEC analysis was performed to study the effect of 5CT on the formation of melittin oligomers. In the absence of 5CT, two peaks were detected at retention times earlier than 10 min (Figure 3c), indicating the existence of molecules greater than 10 kDa (Figure S3). Because the molecular weight of melittin is 2.85 kDa, these peaks were considered to originate from oligomers of melittin. In the presence of 5CT, these peaks decreased and almost disappeared. These results suggested that 5CT prevented the formation of melittin oligomers in solution.

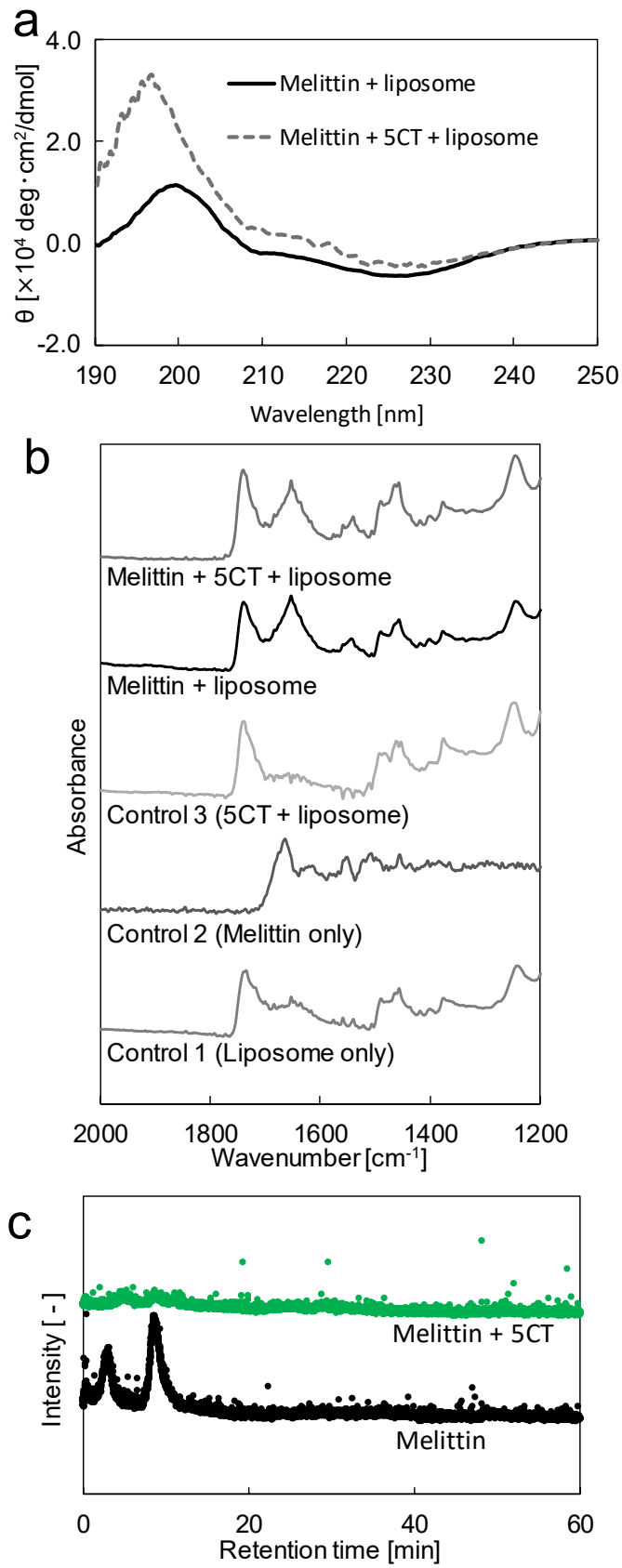

Figure 3 a) CD spectra of melittin solution with and without 5CT. The concentrations of melittin, 5CT,

and liposomes were 5 μM, 50 μM, and 50 μM, respectively. b) ATR-IR spectra of melittin/POPC with and without 5CT. A melittin solution containing POPC liposomes was dried on an ATR plate. The concentrations of melittin, 5CT, and POPC were 50 μM, 500 μM, and 1 mM, respectively. c) Size exclusion chromatograph of melittin solution in the presence and absence of 5CT. The concentrations of melittin and 5CT were 500 μM and 1 mM, respectively.

Visualization of melittin on RBC with an inhibitor

To determine the location of melittin and the inhibitor during hemolysis, we observed the hemolysis of RBCs with and without an inhibitor using CLSM. As shown in Figure 4, TAMRA-melittin was found at the rims of RBCs. Although the addition of D-Trp reduced the fluorescence intensity (fluorescence quenching), melittin was still found at the rims of RBCs. The addition of 5CT almost quenched the fluorescence. Assuming that D-Trp and 5CT inhibited melittin activity in a similar manner, these results indicated that the inhibitor did not affect the localization of melittin on the membranes of RBCs, which agreed with the results of ATR-IR measurements. The fluorescence quenching induced by 5CT suggests that 5CT interacts with melittin.

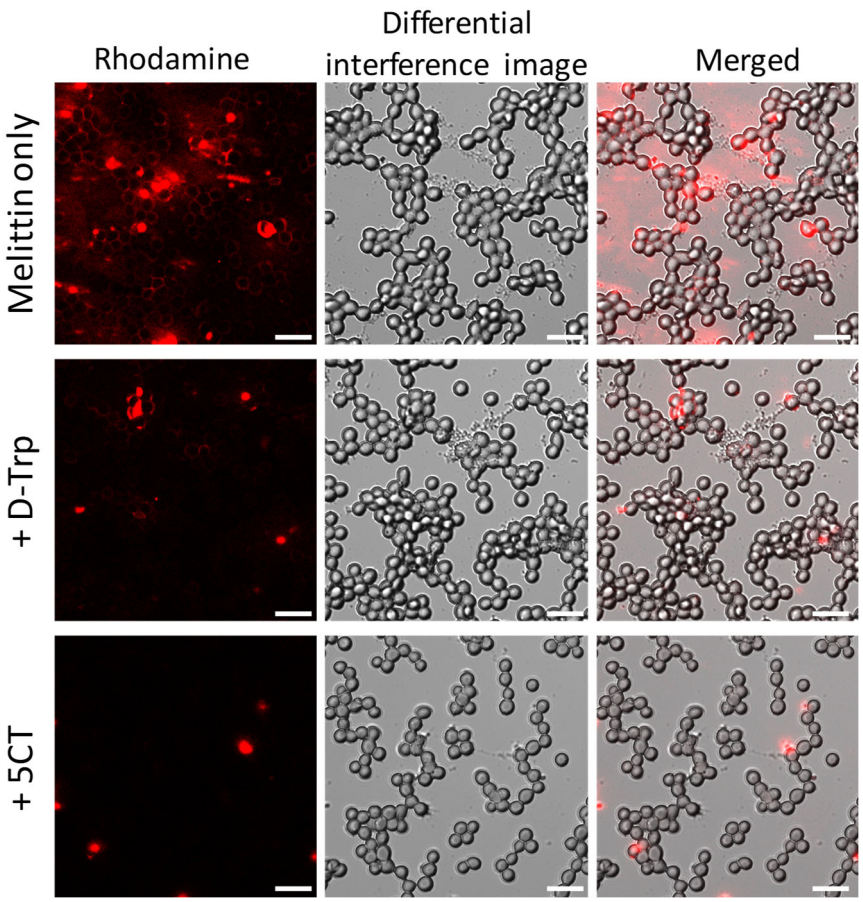

Figure 4 CLSM observation of RBC hemolysis by melittin with and without an inhibitor. The concentrations of melittin, D-Trp, and 5CT were 5 μM, 500 μM, and 500 μM, respectively. Scale bars represent 10 μm.

Molecular interaction between melittin and 5CT

The above results indicate that the indole ring is an important factor in the inhibition of hemolysis induced by melittin. We examined the interaction between 5CT and Trp19 in melittin using fluorescence measurements. In the absence of 5CT, melittin exhibited a fluorescence band at approximately 360 nm (λ_{ex} = 280 nm) (Figure 5a), which originated from Trp19 in melittin. As the 5CT concentration increased, the fluorescence intensity decreased (Figure 4a). These results indicated that 5CT interacted with Trp19 in melittin. Werkmeister et al. reported that hexapeptide inhibitors bind to melittin in the region of Trp19 in melittin.[29]

To examine the kinetics of fluorescence quenching, the Stern–Volmer equation was used:[58, 59]

$$\log \frac{F_0 - F}{F} = \log K_b + n \log[Q] \qquad [1]$$

where [Q] is the concentration of 5CT, n is the number of binding sites, F_0 and F are the steady-state fluorescence intensities of melittin at 360 nm in the absence and presence of 5CT, respectively. K_b is the binding constant between melittin and 5CT. From the best-fit of the Stern–Volmer plot (Figure 5b), the calculated values of n and K_b were 1.4 and 5.0×10^4 [M^{-1}], respectively. Because melittin has only one Trp residue, the calculated number of binding sites (n = 1.4) indicates that Trp19 in melittin and 5CT interacts with each other in a stoichiometric ratio of 1:1 to 1:2. Although the K_b in this experiment was not as high as those of typical antigen-antibody reactions (10^8~10^{12}).

We also conducted a 1H-NMR analysis. 1H-NMR spectra showed chemical shifts at 6.99~7.03 ppm and 7.45~7.48 ppm, which were derived from Trp19 in melittin (Figure 6). These chemical shifts were shifted to the low magnetic field upon the addition of 5CT. These results indicated that there was an interaction between the indole ring of Trp19 in melittin and 5CT.

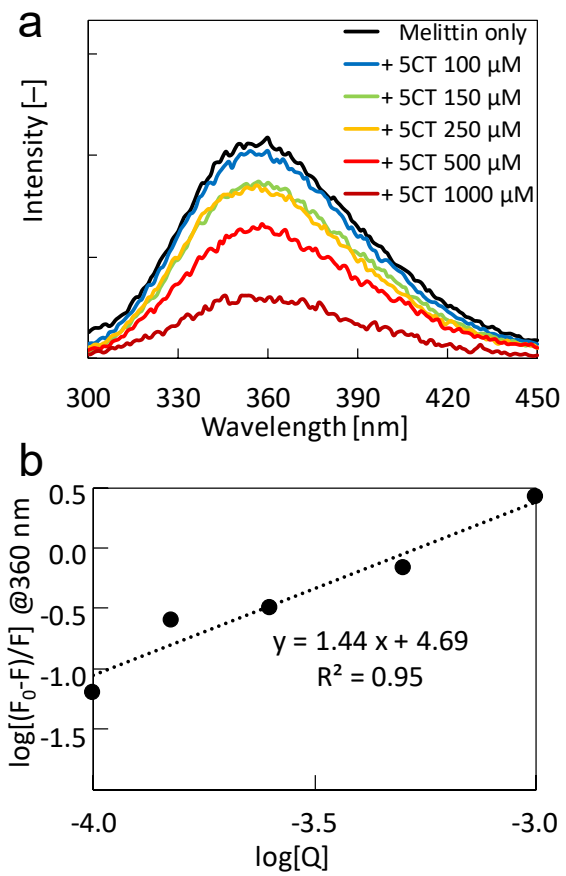

Figure 5 a) Fluorescence spectra of melittin with 5CT at various concentrations (100, 150, 250, 500, and 1000 µM). Melittin (25 µM) was used. b) Stern–Volmer plot for the quenching of intrinsic Trp19 fluorescence of melittin in the presence of 5CT at varied concentrations at 25°C.

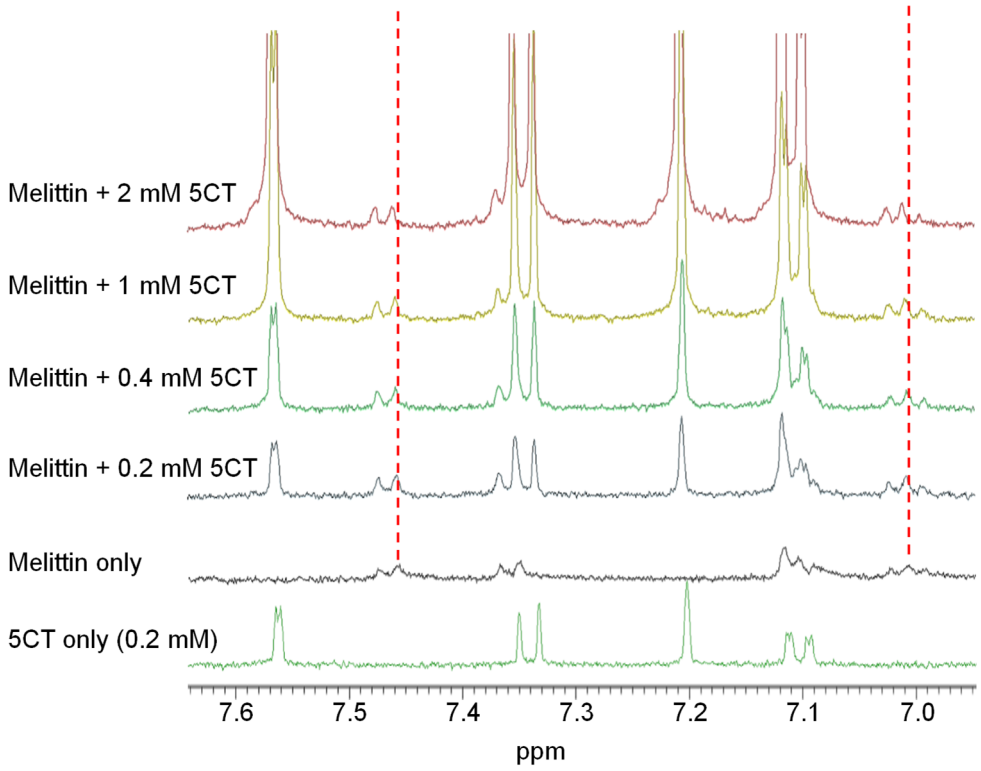

Figure 6 ^{1}H-NMR spectra of 200 μM melittin with 5CT at various concentrations (0.2, 0.4, 1 and 2 mM) in D_2O.

Molecular dynamics (MD) simulation of melittin with 5CT

MD simulation was performed using the Amber molecular dynamics software to investigate the inhibitory effect of 5CT on the formation of melittin tetramers at the atomic level. Four melittin monomers were solvated in a water cubic box with 10-nm edges, and the simulation was carried out at 310 K and 1 atm. The four monomers came together to form a tetramer-like complex after 350 ns at the end of repeated association and dissociation (Figure 7a, c). Figure 7a shows the average distance between the melittin monomers during the calculation. In the absence of 5CT, four melittin monomers formed the complex when the average distance became less than 20 Å after 350 ns, as shown in the snapshot of the molecules at 400 ns (Figure 7c).

When 100 molecules of 5CT were added under the same conditions, four melittin monomers

aggregated with 5CT, and the conformation of the complex stabilized more quickly in the presence than in the absence of 5CT (Figure 7a, d). The small fluctuation in the average distance between the monomers throughout the calculation suggested that the aggregate was stable (Figure 7a). However, the average distance between the monomers with 5CT was larger than that without 5CT after 400 ns. These results indicated that 5CT molecules were intercalated between melittin monomers, which prevented the monomers from assembling with each other. 5CT co-assembled with the melittin monomers to form a complex with a stable conformation, which inhibited the formation of the intrinsic melittin tetramer.

The formation of a melittin tetramer was also monitored by calculating the molecular surface area of melittin. When a melittin complex forms with overlapping molecules, the total surface area of melittin that can be accessed by a solvent molecule decreases. As shown in Figure 7b, the molecular surface area of four melittin monomers decreased over time, indicating the formation of a tetramer. However, in the presence of 100 5CT molecules, the total surface area of melittin did not decrease despite the formation of an aggregate (Figure 7b). These calculations indicated that the distance between melittin monomers in the aggregate was constrained by the intercalation of 5CT between the melittin monomers.

The melittin tetramer is stabilized by hydrophobic interactions between the side chains of hydrophobic amino acid residues of melittin.[60, 61] The Trp residue of melittin plays a key role in stabilizing the conformation of the melittin tetramer because the tryptophan residue is located at a contact point in the crystal structure of the melittin tetramer.[62, 63] The simulation of four melittin monomers without 5CT showed that a pair of Trp side chains were close to each other after 400 ns of calculation (Figure 5c). The aggregation of four melittin monomers in the presence of 5CT resulted in the intercalation of 5CT molecules between the melittin monomers and interacted with the Trp residues, which prevented direct hydrophobic interactions between the Trp side chains (Figure 7d).

Figure S4 shows the magnified view of the melittin tetramer around Trp19 after a 400 ns MD

simulation. This magnified view indicates that there were two different modes of interaction between melittin and 5CT. One was π-π stacking between Trp19 and 5CT (Figure S4a) and the other was cation-π interaction between an amino group of 5CT and an indole ring of Trp19 in melittin (Figure S4b). These interactions between melittin and 5CT were consistent with the experimental hemolysis, fluorescence and 1H-NMR measurements of melittin. These results all supported the importance of the indole rings and amino group. Thus, it was suggested that 5CT prevented the formation of the intrinsic tetramer by 2 different kinds of interactions between 5CT and melittin, inhibiting the hemolytic activity of melittin. Figure S4c and S4d shows that many of amino groups of 5CT were oriented to the outside (to a solvent), which would decrease the melittin's hydrophobicity and affect the interaction between melittin monomers.

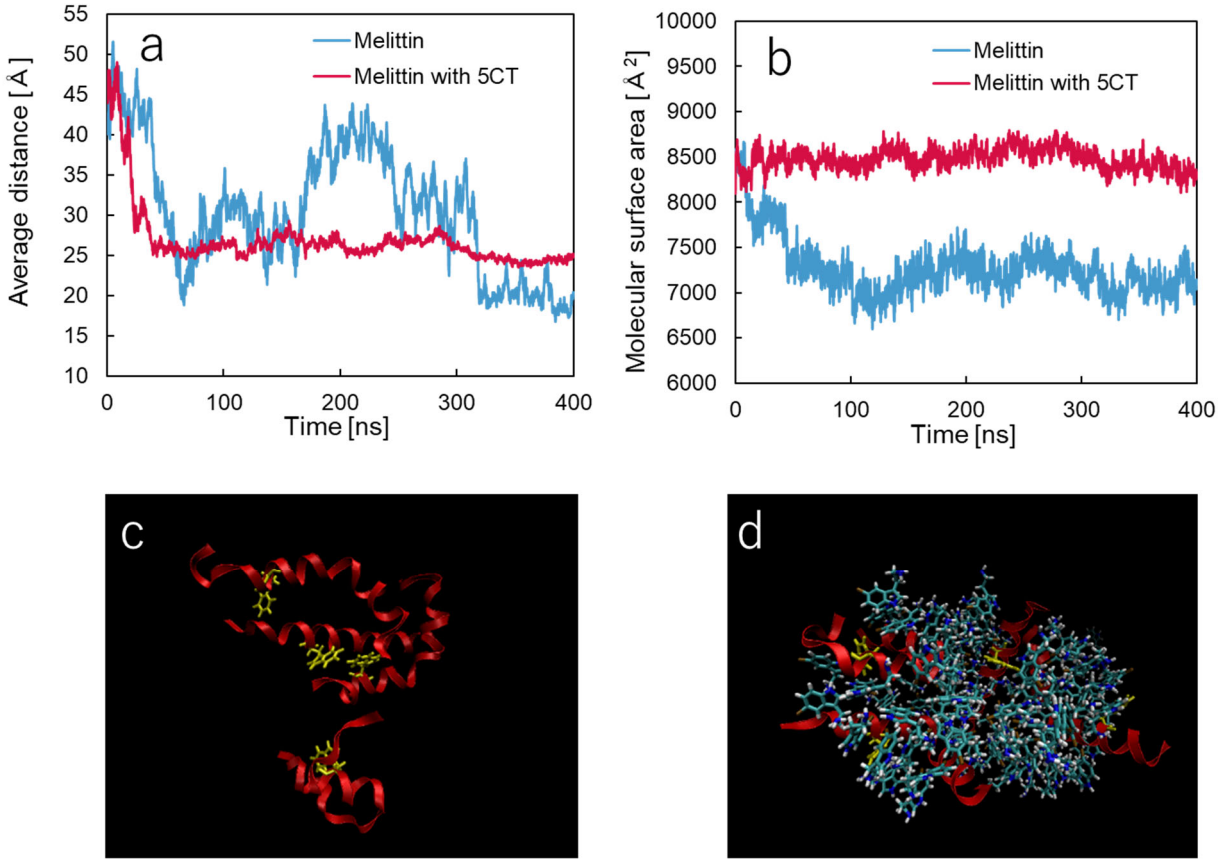

Figure 7 a) Average distance and (b) molecular surface area of four melittin monomers over time in the presence and absence of 5CT calculated from the molecular dynamics simulation. (c, d) Visualized conformation of melittin aggregate after 400 ns of simulation. (c) In the absence and (d) presence of

5CT. Red ribbon: melittin monomer; yellow stick: side chain of tryptophan residue in melittin; multicolored stick: 5CT.

CONCLUSIONS

Inspired by previous studies on the interaction between D-amino acids and L-peptides, we focused on D-amino acids and evaluated the inhibitory effect of D-amino acids on melittin activity. Among the L- and D-amino acids tested, we found that D-Trp acted as an inhibitor of melittin-induced hemolysis. Various Trp derivatives were investigated, and 5CT was found to exhibit the highest inhibitory effect on melittin. Interestingly, many D-Trp-containing dipeptides did not exhibit this remarkable inhibitory effect. The indole ring, amino group, and avoiding steric hindrance of the inhibitor played important roles in the inhibition of melittin activity. Despite the small size and simple molecular structure of 5CT, its IC_{50} was comparable with those of previously studied hexapeptides. Various investigations, including MD simulation, suggested that 5CT interacted with Trp19 in melittin and affected the formation of the melittin tetramer. We are now trying further MD simulation to examine the effect of 5CT on melittin in lipid membranes.

The development of an effective inhibitor as a novel medicine for disease-related proteins is a challenging enterprise. We have presented a rational approach to identify inhibitors using D-amino acids (and their derivatives) by considering the primary structure of the target peptide. This approach can simplify the design of novel inhibitors and streamline the discovery of drug candidates.

ASSOCIATED CONTENT

Supporting Information. Fundamental information (Table S1 and S2) for MD simulations. Additional results (Figure S1-4). This material is available free of charge via the Internet at http://pubs.acs.org.

AUTHOR INFORMATION

Corresponding Author

tmarutcm@crystal.kobe-u.ac.jp

ORCID.org/0000-0003-2428-1911

Notes

The authors declare no competing financial interest.

ACKNOWLEDGMENTS

The authors thank Prof. A. Kondo for technical help with MALDI-TOF/MS. The authors thank Edanz (https://jp.edanz.com/ac) for editing a draft of this manuscript. This study was financially supported by a Grant-in-Aid for Scientific Research on Innovative Areas "Chemistry for Multimolecular Crowding Biosystems" (JSPS KAKENHI Grant No. 20H04711) and by JSPS KAKENHI Grant Numbers 19H05458, 20H02542, 21K18850 and 19K05210. This study was partially supported by Takeda Science Foundation.

REFERENCES

1. Kapetanovic, I. M., Computer-aided drug discovery and development (CADDD): In silico-chemico-biological approach. *Chem. Biol. Interact.* **2008,** *171*, 165-176.
2. Lauria, A.; Tutone, M.; Almerico, A. M., Virtual lock-and-key approach: The in silico revival of Fischer model by means of molecular descriptors. *Eur. J. Med. Chem.* **2011,** *46*, 4274-4280.
3. Lavecchia, A.; Di Giovanni, C., Virtual Screening Strategies in Drug Discovery: A Critical Review. *Curr. Med. Chem.* **2013,** *20*, 2839-2860.
4. Cournia, Z.; Allen, B.; Sherman, W., Relative Binding Free Energy Calculations in Drug Discovery: Recent Advances and Practical Considerations. *J. Chem. Inf. Model.* **2017,** *57*, 2911-2937.
5. Scotti, L.; Mendona, F. J. B.; Ishiki, H. M.; Ribeiro, F. F.; Singla, R. K.; Barbosa, J. M.; Da Silva, M. S.; Scotti, M. T., Docking Studies for Multi-Target Drugs. *Current Drug Targets* **2017,** *18*, 592-604.
6. Wright, P. E.; Dyson, H. J., Intrinsically unstructured proteins: Re-assessing the protein structure-function paradigm. *J. Mol. Biol.* **1999,** *293*, 321-331.
7. Ward, J. J.; Sodhi, J. S.; McGuffin, L. J.; Buxton, B. F.; Jones, D. T., Prediction and functional analysis of native disorder in proteins from the three kingdoms of life. *J. Mol. Biol.* **2004,** *337*, 635-45.
8. Sugase, K.; Dyson, H. J.; Wright, P. E., Mechanism of coupled folding and binding of an intrinsically disordered protein. *Nature* **2007,** *447*, 1021-1025.
9. Uversky, V. N.; Oldfield, C. J.; Dunker, A. K., Intrinsically disordered proteins in human diseases: Introducing the D-2 concept. *Annu. Rev. Biophys.* **2008,** *37*, 215-246.

10. Nasica-Labouze, J.; Nguyen, P. H.; Sterpone, F.; Berthoumieu, O.; Buchete, N. V.; Cote, S.; De Simone, A.; Doig, A. J.; Faller, P.; Garcia, A. *et al.,* Amyloid beta Protein and Alzheimer's Disease: When Computer Simulations Complement Experimental Studies. *Chem. Rev.* **2015,** *115*, 3518-3563.
11. Marsh, J. A.; Singh, V. K.; Jia, Z. C.; Forman-Kay, J. D., Sensitivity of secondary structure propensities to sequence differences between alpha- and gamma-synuclein: Implications for fibrillation. *Protein Sci.* **2006,** *15*, 2795-2804.
12. Linding, R.; Schymkowitz, J.; Rousseau, F.; Diella, F.; Serrano, L., A comparative study of the relationship between protein structure and beta-aggregation in globular and intrinsically disordered proteins. *J. Mol. Biol.* **2004,** *342* 345-353.
13. Theillet, F. X.; Binolfi, A.; Frembgen-Kesner, T.; Hingorani, K.; Sarkar, M.; Kyne, C.; Li, C. G.; Crowley, P. B.; Gierasch, L.; Pielak, G. J.; Elcock, A. H.; Gershenson, A.; Selenko, P., Physicochemical Properties of Cells and Their Effects on Intrinsically Disordered Proteins (IDPs). *Chem. Rev.* **2014,** *114*, 6661-6714.
14. Kamagata, K.; Mano, E.; Itoh, Y.; Wakamoto, T.; Kitahara, R.; Kanbayashi, S.; Takahashi, H.; Murata, A.; Kameda, T., Rational design using sequence information only produces a peptide that binds to the intrinsically disordered region of p53. *Sci. Rep.* **2019,** *9,* 8584.
15. Kolodkin-Gal, I.; Romero, D.; Cao, S. G.; Clardy, J.; Kolter, R.; Losick, R., D-Amino Acids Trigger Biofilm Disassembly. *Science* **2010,** *328,* 627-629.
16. Hochbaum, A. I.; Kolodkin-Gal, I.; Foulston, L.; Kolter, R.; Aizenberg, J.; Losick, R., Inhibitory Effects of D-Amino Acids on Staphylococcus aureus Biofilm Development. *J. Bacteriol.* **2011,** *193*, 5616-5622.
17. Singh, V.; Rai, R. K.; Arora, A.; Sinha, N.; Thakur, A. K., Therapeutic Implication of L-Phenylalanine Aggregation Mechanism and its Modulation by D-Phenylalanine in Phenylketonuria. *Sci. Rep.* **2014,** *4*, 3875.
18. Habermann, E.; Jentsch, J., Sequenzanalyse des Melittins aus den Tryptischen und Peptischen Spaltstücken. *Hoppe-Seyler's Z. Physiol. Chem.* **1967,** *348*, 37-50.
19. Raghuraman, H.; Chattopadhyay, A., Melittin: A Membrane-Active Peptide with Diverse Functions. *Biosci. Rep.* **2007,** *27*, 189-223.
20. Knoppel, E.; Eisenberg, D.; Wickner, W., Interactions of Melittin, A Preprotein Model, with Detergents. *Biochemistry* **1979,** *18*, 4177-4181.
21. Smith, R.; Separovic, F.; Milne, T. J.; Whittaker, A.; Bennett, F. M.; Cornell, B. A.; Makriyannis, A., Structure and Orientation of the Pore-Forming Peptide, Melittin, in Lipid Bilayers. *J. Mol. Biol.* **1994,** *241*, 456-466.
22. Klocek, G.; Schulthess, T.; Shai, Y.; Seelig, J., Thermodynamics of Melittin Binding to Lipid Bilayers. Aggregation and Pore Formation. *Biochemistry* **2009,** *48*, 2586-2596.
23. Dawson, C. R.; Drake, A. F.; Helliwell, J.; Hider, R. C., The Interaction of Bee Melittin with Lipid Bilayer Membranes. *Biochim. Biophys. Acta* **1978,** *510*, 75-86.
24. Brown, L. R.; Braun, W.; Kumar, A.; Wuthrich, K., High Resolution Nuclear Magnetic Resonance Studies of the Conformation and Orientation of Melittin Bound to a Lipid-Water Interface. *Biophys. J.* **1982,** *37*, 319-328.
25. Terwilliger, T. C.; Weissman, L.; Eisenberg, D., The Structure of Melittin in the Form I Crystals and its Implication for Melittin's Lytic and Surface Activities. *Biophys. J.* **1982,** *37*, 353-61.
26. Terwilliger, T. C.; Eisenberg, D., The Structure of Melittin. II. Interpretation of the Structure. *J. Biol. Chem.* **1982,** *257*, 6016-6022.
27. Mihajlovic, M.; Lazaridis, T., Antimicrobial Peptides in Toroidal and Cylindrical Pores. *Biochimica Et Biophysica Acta-Biomembranes* **2010,** *1798*, 1485-1493.
28. Bishop, D. G.; Kenrick, J. R., Melittin: An Inhibitor of Chloroplast Photochemical Reactions. *Biochem. Biophys. Res. Commun.* **1980,** *97*, 1082-1090.
29. Werkmeister, J. A.; Kirkpatrick, A.; McKenzie, J. A.; Rivett, D. E., The Effect of Sequence Variations and Structure on the Cytolytic Activity of Melittin peptides. *Biochim. Biophys. Acta* **1993,**

1157, 50-54.
30. Pinilla, C.; Appel, J. R.; Blondelle, S. E.; Dooley, C. T.; Eichler, J.; Ostresh, J. M.; Houghten, R. A., Versatility of Positional Scanning Synthetic Combinatorial Libraries for the Identification of Individual Compounds. *Drug Dev. Res.* **1994,** *33*, 133-145.
31. Hewish, D.; Werkmeister, J.; Kirkpatrick, A.; Curtain, C.; Pantela, G.; Rivett, D. E., Peptide Inhibitors of Melittin Action. *J. Protein Chem.* **1996,** *15*, 395-403.
32. Blondelle, S. E.; Houghten, R. A.; PerezPaya, E., All D-Amino Acid Hexapeptide Inhibitors of Melittin's Cytolytic Activity Derived from Synthetic Combinatorial Libraries. *J. Mol. Recognit.* **1996,** *9*, 163-168.
33. Blondelle, S. E.; Houghten, R. A.; PerezPaya, E., Identification of Inhibitors of Melittin Using Nonsupport-Bound Combinatorial Libraries. *J. Biol. Chem.* **1996,** *271*, 4093-4099.
34. Lam, Y. H.; Morton, C. J.; Separovic, F., Solid-state NMR Conformational Studies of A Melittin-Inhibitor Complex. *Eur Biophys J* **2002,** *31*, 383-388.
35. Lam, Y. H.; Nguyen, V.; Fakaris, E.; Separovic, F., Conformational Studies of A Melittin-Inhibitor Complex. *J. Protein Chem.* **2000,** *19*, 529-534.
36. Hoshino, Y.; Koide, H.; Urakami, T.; Kanazawa, H.; Kodama, T.; Oku, N.; Shea, K. J., Recognition, Neutralization, and Clearance of Target Peptides in the Bloodstream of Living Mice by Molecularly Imprinted Polymer Nanoparticles: A Plastic Antibody. *J. Am. Chem. Soc.* **2010,** *132*, 6644-6645.
37. Hoshino, Y.; Urakami, T.; Kodama, T.; Koide, H.; Oku, N.; Okahata, Y.; Shea, K. J., Design of Synthetic Polymer Nanoparticles that Capture and Neutralize a Toxic Peptide. *Small* **2009,** *5*, 1562-1568.
38. Hoshino, Y.; Koide, H.; Furuya, K.; Haberaecker, W. W.; Lee, S. H.; Kodama, T.; Kanazawa, H.; Oku, N.; Shea, K. J., The Rational Design of a Synthetic Polymer Nanoparticle that Neutralizes a Toxic Peptide in Vivo. *Proc. Natl. Acad. Sci. U. S. A.* **2012,** *109*, 33-38.
39. Hu, C. M. J.; Fang, R. H.; Copp, J.; Luk, B. T.; Zhang, L. F., A Biomimetic Nanosponge that Absorbs Pore-Forming Toxins. *Nat. Nanotechnol.* **2013,** *8*, 336-340.
40. Lee, H.; Hoshino, Y.; Wada, Y.; Arata, Y.; Maruyama, A.; Miura, Y., Minimization of Synthetic Polymer Ligands for Specific Recognition and Neutralization of a Toxic Peptide. *J. Am. Chem. Soc.* **2015,** *137*, 10878-10881.
41. Winmostar V10, X-Ability Co. Ltd., Tokyo, Japan, 2020.
42. Dewar, M. J. S.; Zoebisch, E. G.; Healy, E. F.; Stewart, J. J. P., The Development and Use of Quantum-Mechanical Molecular-Models .76. Am1 - a New General-Purpose Quantum-Mechanical Molecular-Model. *J. Am. Chem. Soc.* **1985,** *107*, 3902-3909.
43. Case, D. A.; Belfon, K.; Ben-Shalom, I. Y.; Brozell, S. R.; Cerutti, D. S.; Cheatham, T. E.; Cruzeiro, III, V. W. D.; Darden, T. A.; Duke, R. E.; Giambasu, G.; Gilson, M.K. *el al.*, AMBER 2020, University of California, San Francisco. **2020**.
44. Wang, J.; Wolf, R. M.; Caldwell, J. W.; Kollman, P. A.; Case, D. A., Development and Testing of a General Amber Force Field. *J. Comput. Chem.* **2004,** *25*, 1157-1174.
45. Le Grand, S.; Gotz, A. W.; Walker, R. C., SPFP: Speed without Compromise-A Mixed Precision Model for GPU Accelerated Molecular Dynamics Simulations. *Comput. Phys. Commun.* **2013,** *184*, 374-380.
46. Maier, J. A.; Martinez, C.; Kasavajhala, K.; Wickstrom, L.; Hauser, K. E.; Simmerling, C., ff14SB: Improving the Accuracy of Protein Side Chain and Backbone Parameters from ff99SB. *J. Chem. Theory Comput.* **2015,** *11*, 3696-3713.
47. Jorgensen, W. L.; Chandrasekhar, J.; Madura, J. D.; Impey, R. W.; Klein, M. L., Comparison of Simple Potential Functions for Simulating Liquid Water. *J. Chem. Phys.* **1983,** *79*, 926-935.
48. Kusalik, P. G.; Svishchev, I. M., The Spatial Structure in Liquid Water. *Science* **1994,** *265*, 1219-1221.
49. Joung, I. S.; Cheatham, T. E., Determination of Alkali and Halide Monovalent Ion Parameters

for Use in Explicitly Solvated Biomolecular Simulations. *J. Phys. Chem. B* **2008,** *112*, 9020-9041.
50. Schneider, T.; Stoll, E., Molecular-Dynamics Study ff A Three-Dimensional One-Component Model for Distortive Phase Transitions. *Phys Rev B* **1978,** *17*, 1302–1322.
51. Pastor, R. W.; Brooks, B. R.; Szabo, A., An Analysis of the Accuracy of Langevin and Molecular-Dynamics Algorithms. *Mol. Phys.* **1988,** *65*, 1409-1419.
52. Humphrey, W.; Dalke, A.; Schulten, K., VMD: Visual Molecular Dynamics. *J. Mol. Graph. Model.* **1996,** *14*, 33-38.
53. Brauner, J. W.; Mendelsohn, R.; Prendergast, F. G., Attenuated Total Reflectance Fourier-Transform Infrared Studies of the Interaction of Melittin, 2-Fragments of Melittin, and Delta-Hemolysin with Phosphatidylcholines. *Biochemistry* **1987,** *26*, 8151-8158.
54. Ding, B.; Jasensky, J.; Li, Y. X.; Chen, Z., Engineering and Characterization of Peptides and Proteins at Surfaces and Interfaces: A Case Study in Surface-Sensitive Vibrational Spectroscopy. *Acc. Chem. Res.* **2016,** *49*, 1149-1157.
55. Goormaghtigh, E.; Raussens, V.; Ruysschaert, J. M., Attenuated Total Reflection Infrared Spectroscopy of Proteins and Lipids in Biological Membranes. *Biochim. Biophys. Acta Biomembr.* **1999,** *1422*, 105-185.
56. Chen, X. Y.; Wang, J.; Boughton, A. P.; Kristalyn, C. B.; Chen, Z., Multiple Orientation of Melittin inside a Single Lipid Bilayer Determined by Combined Vibrational Spectroscopic Studies. *J. Am. Chem. Soc.* **2007,** *129*, 1420-1427.
57. Sakurai, H.; Nishimura, K.; Yamamoto, S.; Maruyama, T.; Tamura, A., Molecular Design of pH-Responsive Helix Peptides that can Damage Tumor Cells Selectively. *ACS Appl. Bio Mater.* **2021,** *4*, 2442-2452.
58. Anand, U.; Jash, C.; Mukherjee, S., Spectroscopic Probing of the Microenvironment in a Protein-Surfactant Assembly. *J. Phys. Chem. B* **2010,** *114*, 15839-15845.
59. Anand, U.; Jash, C.; Boddepalli, R. K.; Shrivastava, A.; Mukherjee, S., Exploring the Mechanism of Fluorescence Quenching in Proteins Induced by Tetracycline. *J. Phys. Chem. B* **2011,** *115*, 6312-6320.
60. Inagaki, F.; Shimada, I.; Kawaguchi, K.; Hirano, M.; Terasawa, I.; Ikura, T.; Go, N., Structure of Melittin Bound to Perdeuterated Dodecylphosphocholine Micelles as Studied by Two-Dimensional NMR and Distance Geometry Calculations. *Biochemistry* **1989,** *28*, 5985-5991.
61. Qiu, W. H.; Zhang, L. Y.; Kao, Y. T.; Lu, W. Y.; Li, T. P.; Kim, J.; Sollenberger, G. M.; Wang, L. J.; Zhong, D. P., Ultrafast Hydration Dynamics in Melittin Folding and Aggregation: Helix Formation and Tetramer Self-Assembly. *J. Phys. Chem. B* **2005,** *109*, 16901-16910.
62. Blondelle, S. E.; Houghten, R. A., Probing the Relationships Between The Structure and Hemolytic Activity of Melittin With A Complete Set of Leucine Substitution Analogs. *Pept Res* **1991,** *4*, 12-18.
63. Blondelle, S. E.; Simpkins, L. R.; Perez-Paya, E.; Houghten, R. A., Influence of Tryptophan Residues on Melittin's Hemolytic Activity. *Biochim. Biophys. Acta* **1993,** *1202*, 331-336.

TOC Graphic